DALTON
FULL PAPER

The mechanism of olefin exchange in platinum(0) pyridyl–methanimine and pyridyl–thioether complexes. A kinetic study

Luciano Canovese,*[a] Fabiano Visentin,[a] Gavino Chessa,[a] Claudio Santo,[a] Paolo Uguagliati,[a] Lucia Maini[b] and Marco Polito[b]

[a] *Dipartimento di Chimica, Università di Venezia, Calle Larga Santa Marta 2137, 30123 Venice, Italy. E-mail: cano@unive.it*
[b] *Dipartimento di Chimica "G. Ciamician", via Selmi 2, 40126 Bologna, Italy*

Received 12th April 2002, Accepted 19th June 2002
First published as an Advance Article on the web 5th September 2002

The complexes of type [Pt(η^2-ol$_1$)(L–L′)] (ol$_1$ = dimethylfumarate (dmf), naphthoquinone (nq); L–L′ = pyridyl–methanimine (N-N′R′; R′ = Bu^t, 4-MeOC$_6$H$_4$), pyridyl–thioether (N-SR; R = Bu^t, Ph) ligands) were synthesised and fully characterised by means of spectrometric and spectroscopic techniques and elemental analysis. At variance with analogous palladium complexes which display a more complicated solution behaviour, the fluxional rearrangement of pyridyl–thioether platinum(0) olefin substrates occurs *via* inversion at sp^3 sulfur only (L–L′ = N-SR). Moreover, the exchange olefin reactions between [Pt(η^2-ol$_1$)(L–L′)] complexes and the entering olefin ol$_2$ [ol$_2$ = maleic anhydride (ma), fumaronitrile (fn), naphthoquinone (nq) and tetramethylethylenetetracarboxylate (tmetc)] were studied in $CHCl_3$ either under pseudo-first order or second order conditions. On the basis of the ensuing results and of the activation parameters, an associative reaction mechanism is proposed and a novel reactivity scale for the electron poor olefins acting as entering species is determined. The crystal structures of the complexes [Pt(η^2-ol)(L–L′)] (ol = fn, ma, dmf) were also determined and compared with those of analogous platinum(0) and palladium(0) species.

Introduction

Low valent palladium and platinum complexes are often invoked as precursors or active species in several catalytic reactions involving C–C or C–N bond formation.[1] A wealth of papers dealing with Pd(0), Ni(0) and Pt(0) olefin complexes is available, but very few detailed mechanistic studies have appeared in the recent literature.[2] Our research group has been systematically involved in studies on the mechanistic behaviour and the determination of the related equilibrium constants of olefin exchange in Pd(0) substrates containing pyridyl–thioethers and pyridyl–methanimines as ancillary ligands.[3] Our investigations were unfortunately confined mostly to thermodynamic determinations since the high reactivity of the palladium species renders the kinetic studies on olefin exchange reactions difficult. In order to obtain some information on the mechanism of such olefin exchange reactions we had to resort to the use of the bulky tetramethylethylenetetracarboxylate (tmetc) as entering or leaving olefin.[3a,b] The results we obtained, while providing useful information on the intimate olefin exchange mechanism, were necessarily incomplete, being based in the case of pyridyl–thioether complexes on only few reacting species. We therefore decided to extend our studies to the less reactive Pt(0) substrates with the aim to generalise our previous results by the use of several electron poor olefins as nucleophiles. We describe here the synthesis, the reactivity and in some cases the structure of Pt(0) complexes of the type [Pt(η^2-ol)-(L–L′)] which undergo the exchange reaction:

$$[Pt(\eta^2\text{-ol}_1)(L\text{–}L')] + ol_2 \longrightarrow [Pt(\eta^2\text{-ol}_2)(L\text{–}L')] + ol_1 \quad (1)$$

where the ancillary ligand L–L′ represents the pyridyl–thioether or pyridyl–methanimine moiety and ol$_1$ and ol$_2$ are electron poor olefins. To the best of our knowledge this study represents the first kinetic investigation on entering olefins in Pt(0) systems. Moreover, in the case of low valent pyridyl–thioether platinum olefin complexes, the occurrence of inversion of the sulfur's absolute configuration was also investigated, it being the only observable fluxional rearrangement taking place. The complexes characterised and investigated and the employed olefins are reported in the following Scheme 1.

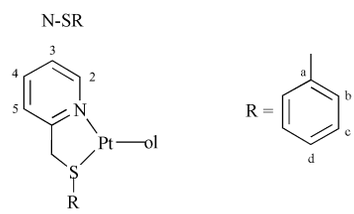

Scheme 1

Results and discussion

1. Synthesis of complexes

Zero valent olefin platinum complexes were synthesised in good yield by reacting Pt(DBA)$_2$ with the appropriate bidentate ligand and the electron-poor olefin in THF. The temperature and reaction time proved very important. With the less

 DOI: 10.1039/b203608h

Table 1 Selected ^{1}H NMR data recorded in $CDCl_3$ at 223 K for platinum(0) olefin pyridyl–thioether complexes (coupling constants in Hz)

Isomeric Complex	Olefinic protons	C–CH_3	O–CH_3	Ratio
[Pt(η^2-dmf)(N–SBu^t)]	3.59 d (J_{HH} = 8.3) 3.24 d (J_{HH} = 8.3)	1.30 s	3.57 s 3.60 s	7 : 1
	3.61 d (J_{HH} = 8.3) 3.26 d (J_{HH} = 8.3)	1.41 s	[a]	
[Pt(η^2-fn)(N–SBu^t)]	2.54 d (J_{HH} = 7.8) 2.94 d (J_{HH} = 7.8)	1.41 s		1.5 : 1
	2.61 d (J_{HH} = 7.8) 2.85 d (J_{HH} = 7.8)	1.39 s		
[Pt(η^2-nq)(N–SBu^t)]	4.32 d (J_{HH} = 6.2) 4.18 d (J_{HH} = 6.2)	1.01 s		1 : 1
	4.39 d (J_{HH} = 6.4) 4.23 d (J_{HH} = 6.4)	1.45 s		
[Pt(η^2-ma)(N–SBu^t)][b]	3.84 d (J_{HH} = 3.7) 3.45 d (J_{HH} = 3.7)	1.31 s		1.75 : 1
	3.78 d (J_{HH} = 3.7) 3.70 d (J_{HH} = 3.7)	1.41 s		
[Pt(η^2-tmetc)(N–SBu^t)][c]		1.36 s	3.62 s 3.61 s	
			3.59 s 3.55 s	

Complexes	Olefinic protons	–CH_3	Isomeric ratio
[Pt(η^2-fn)(N-SMe)]	2.97 d (J_{HH} = 7.8) 2.64 d (J_{HH} = 7.8)	2.58 s	1 : 1
	2.98 d (J_{HH} = 7.9) 2.70 d (J_{HH} = 7.9)	2.41 s	
[Pt(η^2-ma)(N-SMe)]	3.71 d (J_{HH} = 3.7) 3.50 d (J_{HH} = 3.7)	2.38 s	1.2 : 1
	3.81 d (J_{HH} = 3.7) 3.49 d (J_{HH} = 3.7)	2.39 s	

Complexes	Olefinic protons	Isomeric ratio
[Pt(η^2-fn)(N-SPh)]	2.96 d (J_{HH} = 7.9) 2.73 d (J_{HH} = 7.9)	1 : 1
	2.97 d (J_{HH} = 8.1) 2.77d (J_{HH} = 8.1)	
[Pt(η^2-ma)(N-SPh)]	3.81 d (J_{HH} = 3.7) 3.64 d (J_{HH} = 3.7)	1.2 : 1
	3.84 d (J_{HH} = 3.7) 3.64 (J_{HH} = 3.7)	

[a] Obscured. [b] In CD_2Cl_2 at 208 K. [c] In CD_2Cl_2 at 213 K.

hindered olefins the optimised reaction time was 4 h at 45 °C whereas the bulky olefin tmetc requires a reaction time of 24 h at the same temperature; in this case decomposition depresses the yield. The temperature and reaction time applied in the synthesis of each complex are reported in the Experimental.

2. NMR characterisation of complexes

^{1}H and ^{13}C{^{1}H}-NMR spectral data recorded at RT for the complexes are reported in the Experimental, whereas selected ^{1}H NMR data at low temperature are listed in Table 1.

Since the spectral features of the species are strongly influenced by the nature of the coordinated olefin, it is convenient to distinguish among complexes on the basis of the symmetry of the olefin itself which is classified as (*i*) symmetric (tmetc), (*ii*) type *E* (dmf, fn), and (*iii*) type *Z* (ma, nq). However a general feature of the ligands undergoing coordination is a down-field shift of the non-olefinic ligand signals observed either in the ^{1}H or ^{13}C{^{1}H} NMR spectra. In particular, the shifts of H^6 (pyridine ring) in both classes of ligands, the C*H*=N iminic protons in pyridyl–methanimine species and the endocyclic CH_2–S protons in the case of pyridyl–thioether moiety are significant. *H*^{6}, CH_2S and iminic protons also display the characteristic ^{195}Pt satellites. At variance, olefinic protons and carbons upon coordination display a marked high-field shift (3–3.5 and 100–120 ppm respectively) in all the studied substrates. Olefinic protons give rise to an AB system in the case of pyridyl–methanimine species whereas an AX system is detected with pyridyl–thioether complexes. ^{195}Pt satellites are observed in both cases.

2.1. Complexes with symmetric olefins and pyridyl–methanimine ligands. These complexes arise from coordination of a symmetric olefin and of an asymmetric but planar ancillary ligand (C_s symmetry). No chiral centres are therefore detectable in these cases and the substrates are present as unique species.

2.2. Complexes with type *E* olefins and pyridyl–methanimine ligands. These substrates are present in solution as a pair of enantiomers; no symmetry planes are in fact detectable in this case because the coordination of two non equivalent nitrogen atoms and an asymmetric olefin (with substituents above and below with respect to the main coordination plane) induces loss of planarity and consequently chirality on the platinum atom.

2.3. Complexes with type *Z* olefins and pyridyl–methanimine ligands. These complexes are present as a pair of enantiomers since, also in this case, the platinum atom is chiral owing to the asymmetry of the pyridyl–methanimine ligand and the loss of planarity induced by the asymmetric olefin (when coordinated).

2.4. Fluxional behaviour of pyridyl–methanimine complexes. No fluxionality is observed in the case of pyridyl–methanimine complexes since the recorded ^{1}H NMR spectra remain substantially unchanged at any safely attainable temperature.

2.5. Fluxional behaviour of pyridyl–thioether complexes. Scheme 2 represents the diastereoisomers distribution when the pyridyl–thioether species are used as ligands in Pt(0) olefin systems.

The pyridyl–thioether species only undergo sulfur absolute configuration inversion at temperatures comparatively higher than those observed in analogous palladium systems. Apparently, none of the other possible fluxional mechanisms described in previous studies [3b,4] is operative when palladium is replaced by the less reactive platinum.

The spectral features, in the case of inversion at sulfur, are readily explained on the basis of molecular and olefin symmetry.

2.6. Complexes with symmetric olefins and pyridyl–thioether ligands. The ^{1}H NMR spectrum in CD_2Cl_2 of the complex [Pt(η^2-tmetc)(N–S Bu^t)] at 213 K, among other less significant signals, is characterised by the presence of four singlets between 3.50 and 3.65 ppm ascribable to the four different COOCH_3 olefin protons. Meanwhile the endocyclic CH_2-S protons give rise to an AB system between 4.2 and 4.5 ppm, since the presence of the "frozen" sulfur atom (chiral centre) induces diastereotopicity on the thioether protons. At 296 K inversion at sulfur becomes operative, the AB quartet reduces to a singlet at 4.35 ppm (with the platinum satellites becoming evident) and the four singlets turn into two singlets centred at 3.65 ppm.

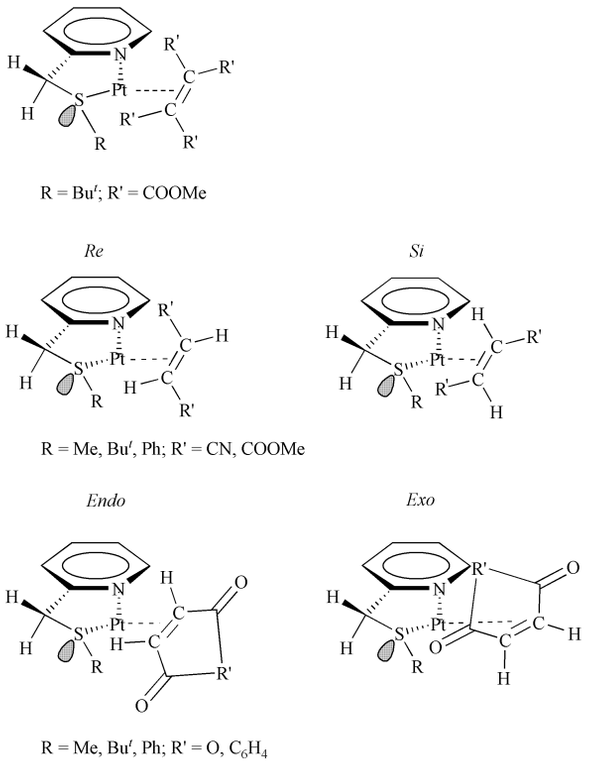

Scheme 2

Inversion at sulfur, which was demonstrated to be independent of the sample concentration, increases the symmetry of the system under study and does not allow anymore the detection of NMR signals due to $COOCH_3$ protons at the same or at the opposite side of the sulfur substituent. Such inversion process is clearly intramolecular in nature and of widespread occurrence in Pd(o) complexes.[3] No hints of further reduction to one singlet of the couple of signals at 3.65 is detected at any attainable temperature; apparently, no olefin rotation or pseudo-rotation mechanisms are observable under our experimental conditions.

2.7. Complexes with type *E* olefins and pyridyl–thioether ligands. According to the isomer distribution reported in Scheme 2, the pyridyl–thioether platinum complexes bearing these olefins (fn, dmf) are present in solution at low temperature as a couple of *Si* and *Re* diastereoisomers. The ^{1}H NMR spectrum in $CDCl_3$ at 223 K of the complex [Pt(η^2-fn)(N–S Bu^t)] is readily interpretable on the basis of this situation. Fig. 1a shows selected regions of the spectrum in which the olefinic protons are detected as two pairs of AX doublets (2.5–3.0 ppm) ascribable to the two different diastereoisomers present in solution at different concentrations. The same difference in population is confirmed in the region of *t*-butyl protons, $C(CH_3)_3$, at 1.4 ppm. The two singlets are again clearly attributable to the two isomers *Si* and *Re*. Increasing the temperature to 296 K promotes inversion at sulfur and the concomitant spectral simplification (Fig. 1b). Again, further increments in the temperature do not induce other fluxional rearrangements. As a matter of fact, in this case olefin rotation would leave the absolute configuration of the platinum atom unchanged and the spectrum of the substrate would display only one signal in the region of olefinic protons but the persistence of an AB system ascribable to CH_2S protons which would remain diastereotopic because of the chirality of the metal centre.[3b]

2.8. Complexes with type *Z* olefins and pyridyl–thioether ligands. Complexes bearing *Z* olefins (ma, nq) give rise two diastereoisomers (*endo*, *exo*) together with their undetectable enantiomers (Scheme 2). The presence of the two diastereoisomers in different concentrations is clearly detectable in the

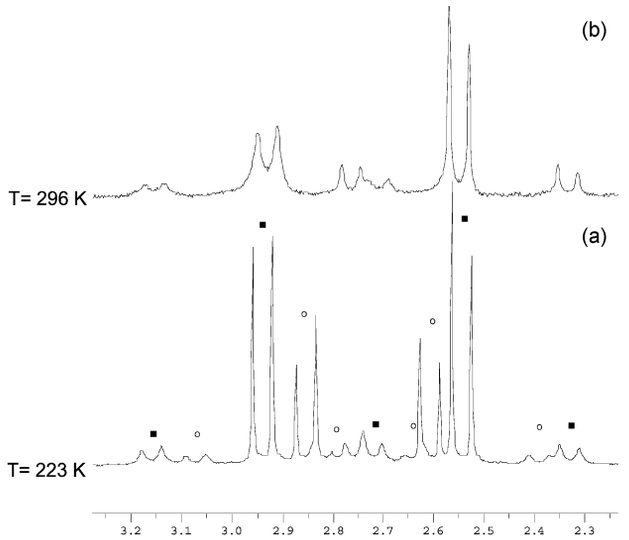

Fig. 1 Olefinic protons in the ^{1}H NMR spectrum of the complex [Pt(η^2-fn)(N–SBu^t)] in $CDCl_3$ at 223 (a) and 296 K (b).

low temperature spectrum, while inversion at sulfur simplifies the spectrum by increasing the complex symmetry since such rearrangement corresponds to an effective interchange between diastereoisomers.

As can be seen, diastereoisomers, when present, are often in different concentrations. This peculiarity probably arises from the mutual steric hindrance generated between bulky substituent groups at the olefin and at the sulfur lying on the same side of the main coordination plane.

3. Determination of olefin exchange rates

The rates of olefin exchange [reaction (1)] were determined by means of a conventional UV/vis spectrophotometer equipped, when necessary, with a rapid mixing device. The spectral changes of the reaction mixture, obtained by mixing appropriate micro-aliquots of entering olefin with a pre-thermostatted solution of the complex under study, were monitored at constant temperature (25 °C) in the range 330–450 nm. At variance with the analogous reactions of palladium pyridyl–thioether and pyridyl–methanimine olefin species, no equilibrium reactions could be observed when palladium is replaced with the less reactive platinum. Moreover, the reaction rates considerably decrease so that a wider number of exchanging complexes and olefins could be studied. The results of such an investigation are summarised in Table 2.

In order to ensure a suitable change in absorbance only naphthoquinone and dimethylfumarate were used as leaving olefins. In particular, naphthoquinone proved the more versatile species thanks to its chromophoric properties but also because the rates of displacement of this olefin are more accessible. The reactivity of its complexes is in fact somewhat lower than that of those bearing dimethylfumarate; moreover, in some cases dmf complexes prevent the determination of the rate constants in the case of the slower reactions involving tmetc since they undergo extensive decomposition or do not show detectable changes in absorbance.

In almost all the cases examined, the observed rate law is:

$$\text{rate} = k_2[\text{complex}][\text{ol}_2] \quad (2)$$

The k_2 values (Table 2) for the slower reactions were determined by regression analysis of the relationship

$$k_{obs} = k_2[\text{ol}_2] \quad (3)$$

under pseudo-first order conditions (excess of ol_2), where k_{obs} was derived from fitting a monoexponential reaction profile.

Table 2 Second order rate constants for the reaction $[Pt(\eta^2\text{-}ol_1)(L\text{–}L')] + ol_2 \longrightarrow [Pt(\eta^2\text{-}ol_2)(L\text{–}L')] + ol_1$ in $CHCl_3$ at 25 °C

Complex	k_2 for ol_2/mol^{-1} dm^3 s^{-1}			
	ma	fn	nq	tmetc
[Pt(η²-nq)(N–SBu^t)]	224 ± 6[a]	40 ± 2[c]		[d]
[Pt(η²-dmf)(N–SBu^t)]	[b]	1709 ± 15[a]	1023 ± 5[a]	[e]
[Pt(η²-nq)(N-SPh)]	[b]	451 ± 6[a]		$(5.8 \pm 0.2) \times 10^{-3}$[f]
[Pt(η²-nq)(N-N′C_6H_4OMe-4)]	[b]	[b]		$(2.1 \pm 0.1) \times 10^{-2}$[f]
[Pt(η²-nq)(N-N′Bu^t)]	1383 ± 23[a]	344 ± 1[a]		[d]
[Pt(η²-dmf)(N-N′C_6H_4OMe-4)]	[b]	[b]	[b]	0.27 ± 0.01[g]

[a] Measured under second order conditions. [b] Too fast to measure. [c] Measured under pseudo-first and second order conditions. [d] Too slow to measure (decomposition). [e] No detectable changes in absorbance among reactants and products. [f] Measured under pseudo-first order conditions. [g] See text.

For the faster reactions, k_2 values were computed from direct analysis of absorbance data *vs.* time according to the customary second order treatment ([complex] ≈ [ol_2]). The experimental data provide no evidence for the contribution of an olefin-independent, first order path to the overall reaction rates. In fact, the plots of k_{obs} *vs.* [ol_2] show no statistically significant intercept, whereas under second order conditions *bona fide* k_1 contributions, if any, would be masked by the manifold sources of experimental error related to uncertainties in the initial reactant concentrations combined with numerical uncertainties in the fitting procedure arising from correlations between the fitted parameters.

It can be shown that the reaction profile for a mixed first-second order process

$$Pt(ol_1) + ol_2 \longrightarrow Pt(ol_2) + ol_1\ k_2$$

$$Pt(ol_1) \longrightarrow Pt + ol_1\ k_1$$

$$Pt + ol_2 \longrightarrow Pt(ol_2)\ \text{fast}$$

is given by

$$[Pt(ol_1)]_t = M_0\,[k_1 + k_2(ol_0 - M_0)]/((k_1 + k_2 ol_0)\exp\{t[k_1 + k_2(ol_0 - M_0)]\} - k_2 M_0)$$

where $M_0 = [Pt]_0$, $ol_0 = [ol_2]_0$.

The k_1 and k_2 rate constants can in principle be determined by fitting concentration (or any instrumental response that is proportional to concentration, such as absorbance *etc.*) to time data by non-linear regression, with k_1 and k_2 being the parameters to be optimised. In practice, however, the results rely heavily on the knowledge of the precise values of M_0 and ol_0 (which may not be known with the desired accuracy in diluted solutions) and the iterative convergence process is affected by the high correlation between the parameters fitted. This situation gives rise to large standard errors of estimate for the parameters and to the difficulty of discriminating between the mixed first–second order model and a purely second order path ($k_1 \approx 0$) when the first order one does not make a substantial contribution to the overall mechanistic picture. Such is the situation prevailing in the present work in which even residual analysis (a customary tool of the trade in evaluating the adequacy of a given model in regression analysis) provided no significant support to the contention that the reactions studied herein proceed by a path more complicated than a purely second order mechanism. This is consistent both with the lack of an olefin-independent term in the rate law determined under pseudo-first order conditions and with our previous experience on related olefin exchange processes involving palladium complexes with bidentate ligands. On the other hand, a change in mechanism on going from first- to second order conditions, albeit possible, is not supported by any observable data, and we prefer to stick to the old prescription that there is no merit in choosing a mechanism more complicated than that demanded by experimental evidence.

As a matter of fact, a second order treatment would be able to reveal a first order path only when the latter contributes substantially to the overall rate, which is not our case. Moreover, our experience in this field strongly supports the view that the contribution of a first order (either dissociative or solvento-mediated) path is to be ruled out in the case of these well known bidentate ligand complexes, it only being observed when terdentate species are involved.[3c] Consistently, for the reaction of [Pt(η²-nq)(N–S Bu^t)] with fn, for which both data treatments are feasible, the computed k_2 values for the two approaches are superimposable within experimental error.

This reaction was also studied at variable temperature and the rate constants k_2 determined in the range 15–40 °C were analysed according to a re-parameterised Eyring–Polanyi equation.[5] The ensuing activation parameters were $\Delta H^{\neq}$ = 7.0 ± 0.3 Kcal mol^{-1} and $\Delta S^{\neq}$ = −28 ± 1 cal mol^{-1} K^{-1}. In particular the low activation enthalpy and the largely negative entropic value strongly suggest an associative pathway for these olefin exchange reactions. As a matter of fact, the resulting 18-electron activated complex was proposed to govern the activation process occurring in analogous reactions involving palladium complexes.[3a,b]

As can be seen the k_2 values in Table 2 span an interval of almost six orders of magnitude, indicating the prominent influence of steric requirements of the entering olefin. The predominant features which emerge from analysis of the data in Table 2 might be summarised by the following points:

(i) Within homologous series the *t*-butyl substituent at sulfur or at iminic nitrogen imparts a lower reactivity to the corresponding complexes than the phenyl or 4-OMeC_6H_4 group.

(ii) The reactivity of the pyridyl–thioether complexes is lower than that of the corresponding pyridyl–methanimine species.

(iii) Dimethylfumarate is a better leaving group than naphthoquinone.

(iv) The reactivity order of the entering olefin is : ma > fn ≈ nq ⩾ tmetc.

The first and second point can be easily discussed on taking into consideration the associative nature of the reaction which is expected to be strongly influenced by the steric hindrance of the reagents. The bulkiness of the *t*-butyl group with respect to the phenyl fragment depresses the substitution reaction rate to a larger extent than its electronic characteristics would be expected to do. It was in fact shown that in substitution reactions between olefins in pyridyl–thioether palladium systems, the difference in reactivity due to electronic reasons between groups with analogous steric hindrance (Pr^i and Ph) was always smaller than one order of magnitude, whereas the rate constants can increase by more than three orders of magnitude if the bulky *t*-butyl substituent at sulfur is replaced by the methyl group.[3b] Analogously, the difference in reactivity among complexes bearing the same substituent at sulfur or at iminic nitrogen can be traced back to the peculiar behaviour of the sp^3 sulfur which, at room temperature, rapidly inverts its absolute configuration, pushing the substituent up or down with respect to the main coordination plane, thereby inducing some sort of

permanent steric retardation. Again, no particular differences in the electronic properties among pyridyl–thioether and pyridyl–methanimine ligands were found in equilibrium studies in which the latter were replaced by the former and *vice versa*.[3b] Apparently, the π-antibonding orbitals of the sp^2 iminic nitrogen behave similarly to the free d orbitals of the sp^3 sulfur atom since they are comparable in determining the extent of π-bond back-donation. As for point three, according to the data reported in Table 2 the dmf complex studied seems to be more labile than the analogous nq, at variance with previous results determined in palladium systems where dmf derivatives proved less reactive than those bearing nq, essentially for entropic reasons.[3a] However, accurate analysis of kinetic data suggests a different interpretation for the reaction involving the complex [Pt(η²-dmf)(N-N′C_6H_4OMe-4)] with tmetc. The reaction profile could be described as two consecutive steps leading to the final species [Pt(η²-tmetc)(N-N′C_6H_4OMe-4)], as can be shown by the superimposability of the spectrum of a solution of an authentic sample of [Pt(η²-tmetc)(N-N′C_6H_4OMe-4)] with that of the final reaction mixture at the same concentration. Since we are dealing with two consecutive reactions, some sort of stable intermediate species will accumulate before formation of the products. Owing to the low activation enthalpy required by these reactions we suggest the formation of an intermediate bearing both the entering and the leaving olefin which can either give the final species or revert to the initial one. This situation is described by eqn. (4).

The customary approach to this problem[6] allows the determination of only k_2 by the regression analysis of $(\lambda_1 + \lambda_2)$ *vs.* $[ol_2]$ where λ_1 and λ_2 are the observed combinations of constants calculated by treating the above scheme by a bi-exponential model. The sum of $k_1 + k_{-1}$ (which is given as the intercept of the linear regression analysis) does not allow separation of the two terms; however, the resulting value ($k_1 + k_{-1} = (1.53 \pm 0.01) \times 10^{-2}\ s^{-1}$) suggests that since the overall dissociative path is slow the predominant part of the sum can be traced back to the dissociation of dmf (k_{-1}) which is by far the less coordinating olefin.

Point four takes into account the different reactivity order among entering olefins which, to the best of our knowledge, was never determined before. At variance, the thermodynamic stability induced by these electron poor alkenes was measured in the case of Pd(0) substrates and was ascribed to the electron-withdrawing capability of olefin substituents since the π-back-donation from the metal to the alkene is assumed to be the most important contribution to the overall bond strength.[2a] From the kinetic point of view, the electron-withdrawing ability of alkene substituents always plays an important role, but it is the steric hindrance of the entering olefin that dictates its reactivity, thereby overwhelming any other effect. As a matter of fact, ma proved the most efficient olefin since its electronic features are coupled with its modest *Z*-symmetry modulated steric demand, which would drive the attack through the unsubstituted side of the olefin. Analogously, nq reacts almost as efficiently as fn, although the latter results much more favoured from the electronic point of view, as is shown by the high equilibrium constants for olefin displacement by fn observed in related systems.[3] The case of tmetc is paradigmatic of the importance of steric requirements. Although no direct evidence is available, from a cross extrapolation of the existing rate constants ma results about six orders of magnitude more efficient than tmetc. The ratio between these olefin displacement equilibrium constants for Pd(0) systems was shown to be confined well within four orders of magnitude,[3a,b] indicating that the electronic properties represent a minor contribution to the overall rate constants. Since our conclusions take often into account experimental results that we obtained with analogous palladium systems, one may argue that direct comparison would not be warranted. However, it may be easily shown that the complexes [M(η²-nq)(N-N′C_6H_4OMe-4)] and [M(η²-nq)-(N-SPh)] display a similar reactivity trend when they react with tmetc independently of the metal (M = Pt, Pd), the ratios between rate constants being 3.6 and 2 when M = Pt and Pd, respectively. Apart some sort of levelling effect, the comparison seems feasible. Platinum(0) complexes display a reactivity to substitution which is three orders of magnitude less than that of the corresponding palladium systems, thus confirming that also in the case of low oxidation states the difference between platinum and palladium is maintained.

4. X-Ray diffraction study

The molecular structures of complexes [Pt(η²-ol)(N-N′Bu^t)] (ol = fn, ma, dmf) have been confirmed by X-ray crystallography. The ORTEP diagrams are shown in Fig. 2, 3 and 4 while the selected bond distances and angles are listed in Table 3.

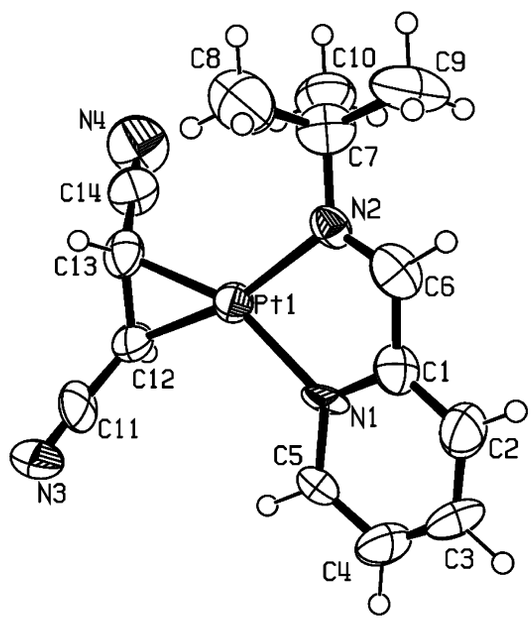

Fig. 2 ORTEP representation of [Pt(η²-fn)(N-N′Bu^t)] complex.

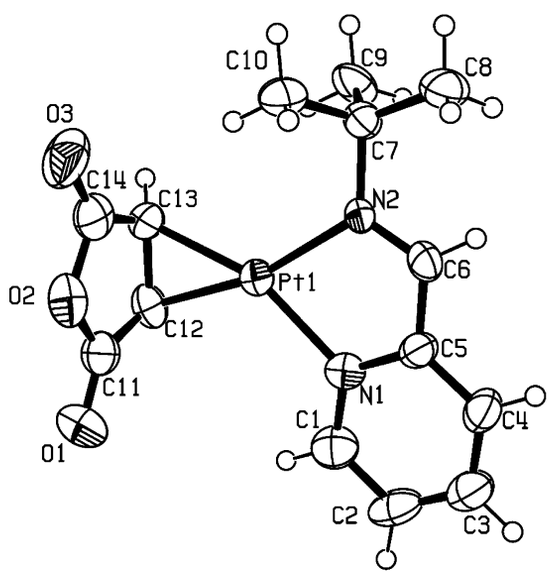

Fig. 3 ORTEP representation of [Pt(η²-ma)(N-N′Bu^t)] complex.

$$[Pt(\eta^2\text{-}ol_1)(L\text{-}L')] \underset{k_{-1}}{\overset{k_2[ol_2]}{\rightleftharpoons}} [Pt(ol_1)(ol_2)(L\text{-}L')] \xrightarrow{k_1} [Pt(\eta^2\text{-}ol_2)(L\text{-}L')] + ol_1 \quad (4)$$

Table 3 Selected bond lengths (Å) for [Pt(η²-fn)(N-N′Bu^t)], [Pt(η²-ma)(N-N′Bu^t)] and [Pt(η²-dmf)(N-N′Bu^t)]

	[Pt(η²-fn)(N-N′Bu^t)]		[Pt(η²-ma)(N-N′Bu^t)]		[Pt(η²-dmf)(N-N′Bu^t)]	
Pt–C	Pt(1)–C(12)	2.007(15)	Pt(1)–C(12)	2.018(7)	Pt(1)–C(14)	2.044(9)
	Pt(1)–C(13)	2.014(14)	Pt(1)–C(13)	2.061(6)	Pt(1)–C(13)	2.052(9)
					Pt(2)–C(30)	2.043(7)
					Pt(2)–C(29)	2.049(8)
C=C	C(12)–C(13)	1.43(2)	C(12)–C(13)	1.449(11)	C(13)–C(14)	1.465(12)
					C(29)–C(30)	1.436(12)
Pt–N	Pt(1)–N(1)	2.105(15)	Pt(1)–N(1)	2.082 (6)	Pt(1)–N(1) 2.094(7)	
	Pt(1)–N(2)	2.134(12)	Pt(1)–N(2)	2.101(5)	Pt(1)–N(2)	2.107(7)
					Pt(2)–N(3)	2.081(7)
					Pt(2)–N(4)	2.125(6)

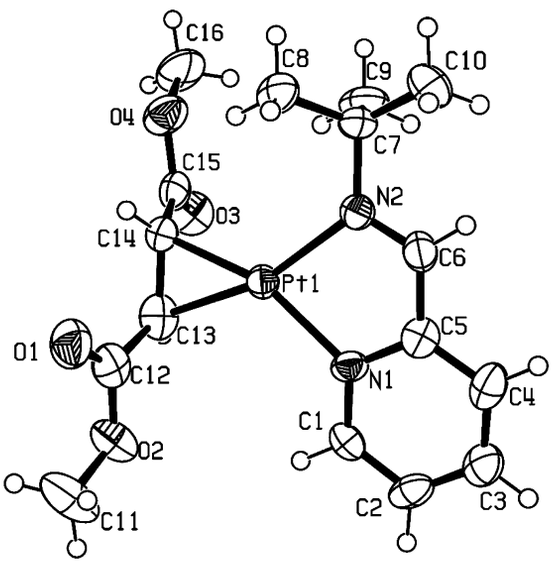

Fig. 4 ORTEP representation of [Pt(η²-dmf)(N-N′Bu^t)] complex. Only one of the two independent molecules is shown.

In all complexes the platinum(0) has a planar geometry. Two sites of coordination are occupied by the bidentate ligand N-N′Bu^t while the other positions are occupied by the double bond of the olefin. In the CSD (October 2001) only one crystal structure with Pt(0) coordinated to nitrogen and olefin is reported.[7] In all complexes described in this article the Pt(0)–N distances are influenced by the nature of the nitrogen atom. In fact, the pyridine nitrogen is closer to the Pt than the imine one (see Table 3). The Pt(0)–C distances show differences among the complexes, however they are slightly shorter than the complexes with P-donors. Complexes with Pt(0) olefin and S-donors are not present in the CSD. Pt(0) in [Pt(η²-fn)(N-N′Bu^t)] has the shortest distances (2.007(15) and 2.014(14) Å), in [Pt(η²-ma)-(N-N′Bu^t)] the Pt–C interactions exhibit a higher degree of asymmetry than in [Pt(η²-fn)(N-N′Bu^t)] and [Pt(η²-dmf)-(N-N′Bu^t)], Pt(1)–C(12) is 2.018(7) Å, comparable with the interaction in [Pt(η²-fn)(N-N′Bu^t)], while Pt(1)–C(13) is 2.061(6) Å – the longest interaction observed in the complexes reported. The average value 2.040 is comparable with those observed in [Pt(η²-dmf)(N-N′Bu^t)]. The crystal structure of [Pt(η²-dmf)(N-N′Bu^t)] shows two independent molecules. The distances Pt–C are comparable in the two independent molecules and are in the range of 2.043–2.052Å. In the complex [Pt(η²-dmf)(dmphen)] reported by Albano *et al.*[8] the Pt–C distances are quite asymmetric (1.88(3) and 2.09(2)) but the average value (1.99) is significantly shorter than that found in [Pt(η²-dmf)(N-N′Bu^t)]. Consequently the average C=C bond length in the latter is higher than that found in [Pt (η²-dmf)-(dmphen)] (1.450 *vs.* 1.420 Å, respectively). Moreover the C=C bond distance in the complex [Pt(η²-ma)(N-N′Bu^t)] appears to be significantly longer than those found in all the analogous maleic anhydride platinum and palladium compounds.[1p,2a,3b] The average Pt–C length in the case of the two complexes bearing the two class *E* olefins (fn, dmf) increases significantly on going from [Pt(η²-fn)(N-N′Bu^t)] to [Pt(η²-dmf)(N-N′Bu^t)], (2.011 *vs.* 2.047 Å, respectively) thereby supporting the increased kinetic lability of the latter with respect to all the Pt(0) complexes studied in this work.

Experimental

Preparation of ligands

The pyridyl–thioether (N-SR)[9] and pyridyl–methanimine (N-N′R′)[10] ligands were prepared according to published procedures. All other chemicals were commercial grade and were purified or dried, where required, by standard methods.[11]

Preparation of complexes

All the complexes described herein were obtained by analogous synthetic procedures. Therefore we report the detailed preparation of only one species. We however indicate analytical and spectroscopic data together with the temperature and the time of reaction for each substrate obtained. In particular the latter are of paramount importance in obtaining pure samples since the slower reactions lead often to extensive decomposition with concomitant formation of platinum metal and the optimised yield depends on a carefully balanced choice between time and reaction temperature.

[Pt(η²-ma)(N-SBu^t)]. To a solution of 0.206 g (0.31 mmol) of $Pt(DBA)_2$[12] in anhydrous THF, 0.0343 g (0.34 mmol) of maleic anhydride (ma) and 0.3387 g (0.34 mmol) of N–SBu^t ligand were added under inert atmosphere (N_2). The resulting reaction mixture was stirred for 24 h at 45 °C under nitrogen and the initial deep violet colour turned to yellowish. The solution was dried under reduced pressure, re-dissolved in CH_2Cl_2, treated with activated charcoal and filtered on celite filter. Reduction under small volume and addition of diethyl ether yielded 0.0775 g (0.16 mmol, 53% yield) of the title complex as cream-coloured microcrystals (t_{react} 24 h at 45 °C).

Found: C, 35.52; H, 3.74; N, 3.07; S, 6.52. $C_{14}H_{17}NO_3PtS$ requires: C, 35.44; H, 3.61; N, 2.95; S, 6.76.

IR (KBr pellets, cm^{-1}): $\nu_{C=N}$ 1603 (m); $\nu_{C=O}$ 1730, 1793.

^{1}H NMR (in $CDCl_3$, RT), δ (ppm): CH_3 1.42 (9H, s); *H*C=C*H* 3.55 (H, d, J = 3.7 Hz, J_{H-Pt} = 82.2 Hz); *H*C=C*H* 3.87 (H, d, J = 3.7 Hz, J_{H-Pt} = 82.2 Hz); CH_2S 4.32 (2H, m); H^5 7.27 (H, m); H^3 7.64 (H, d, J = 7.7 Hz); H^4 7.94 (H, td, J = 7.7 Hz, J = 1.5 Hz); H^6 9.17 (H, d, J = 5.5 Hz, J_{H-Pt} = 30 Hz).

[Pt(η²-fn)(N-SBu^t)]. Cream-coloured microcrystals (69% yield; t_{react} 4.5 h at 45 °C or 17 h at RT).

Found: C, 37.12; H, 3.86; N, 9.29; S, 7.25. $C_{14}H_{17}N_3PtS$ requires: C, 37.00; H, 3.77; N, 9.25; S, 7.06.

IR (KBr pellets, cm^{-1}): $\nu_{C=N}$ 1604 (m); $\nu_{C=N}$ 2202 (s).

^{1}H NMR (in $CDCl_3$, RT), δ (ppm): CH_3 1.48 (9H, s); *H*C=C*H* 2.62 (H, d, J = 7.7 Hz, J_{H-Pt} = 85.9 Hz); *H*C=C*H* 3.00 (H, d, J = 7.7 Hz, J_{H-Pt} = 88.6 Hz); CH_2S 4.36 (2H, m); H^5 7.30 (H, dd,

J = 7.7 Hz, J = 4.75 Hz); H^3 7.66 (H, d, J = 8.4); H^4 7.97 (H, td, J = 7.7 Hz, J = 1.8 Hz); H^6 9.22 (H, d, J = 4.75 Hz, J_{H-Pt} = 30.3 Hz).

^{13}C NMR (in $CDCl_3$, RT), δ (ppm): H*C*=*C*H 4.04 (J_{C-Pt} = 420.5 Hz); H*C*=*C*H 9.63 (J_{C-Pt} = 410.3 Hz); C–(*C*H$_3$)$_3$ 29.9 (J_{C-Pt} = 21.5 Hz); *C*H$_2$S 41.2 (J_{C-Pt} = 24.9 Hz); *C*–(CH$_3$)$_3$ 50.9; *C*≡N 122.0; C^5 123.5 (J_{C-Pt} = 30.0 Hz); C^3 125.1 (J_{C-Pt} = 34.0 Hz); C^4 138.8; C^6 154.97 (J_{C-Pt} = 45.2 Hz); C^2 160.9.

[Pt(η^2-dmf)(N-SBu^t)]. Cream-coloured microcrystals (53% yield; t_{react} 4 h at 45 °C or 17 h at RT).

Found: C, 36.85; H, 4.58; N, 2.87; S, 6.28. $C_{16}H_{23}NO_4PtS$ requires: C, 36.92; H, 4.45; N, 2.69; S, 6.16.

IR (KBr pellets, cm^{-1}): $\nu_{C=O}$ 1686 (s); $\nu_{C=N}$ 1603 (m).

^{1}H NMR (in $CDCl_3$, RT), δ (ppm): C*H*$_3$ 1.41 (9H, s); OC*H*$_3$ 3.60 (3H, s); OC*H*$_3$ 3.65 (3H, s); *H*C=C*H* 3.56 (H, d, J = 8.4 Hz, J_{H-Pt} = 89.5 Hz); *H*C=C*H* 3.85 (H, d, J = 8.4 Hz, J_{H-Pt} = 88.4 Hz); C*H*$_2$S 4.27 (2H, m); H^5 7.22 (H, m); H^3 7.56 (H, d, J = 8.4); H^4 7.86 (H, td, J = 7.7 Hz, J = 1.5 Hz); H^6 9.23 (H, d, J = 5.5 Hz, J_{H-Pt} = 30.3 Hz).

^{13}C NMR (in $CDCl_3$, RT), δ (ppm): H*C*=*C*H 28.14 (J_{C-Pt} = 375.3 Hz); H*C*=*C*H 35.04 (J_{C-Pt} = 344.7 Hz); C–(*C*H$_3$)$_3$ 29.56 (J_{C-Pt} = 21.5 Hz); *C*H$_2$S 41.10 (J_{C-Pt} = 26.0 Hz); *C*-(CH$_3$)$_3$ 49.70; OC*H*$_3$ 50.96; OC*H*$_3$ 50.74; C^5 123.1 (J_{C-Pt} = 26.0 Hz); C^3 124.6 (J_{C-Pt} = 35.0 Hz); C^4 137.90; C^6 154.10 (J_{C-Pt} = 45.9 Hz); C^2 160.77; *C*=O 174.65: *C*=O 176.67.

[Pt(η^2-nq)(N-SBu^t)]. Light-brown microcrystals (48% yield; t_{react} 4 h at 45 °C or 17 h at RT).

Found: C, 44.77; H, 3.84; N, 2.81; S, 6.23. $C_{20}H_{21}NO_2PtS$ requires: C, 44.94; H, 3.96; N, 2.62; S, 6.00.

IR (KBr pellets, cm^{-1}): $\nu_{C=O}$ 1637 (s), 1625 (s); $\nu_{C=N}$ 1589(m).

^{1}H NMR (in $CDCl_3$, RT), δ (ppm): C*H*$_3$ 1.25 (9H, s); C*H*$_2$S 4.18 (2H, m); *H*C=C*H* 4.38 (H, d, J = 6.2 Hz, J_{H-Pt} = 70.9 Hz); *H*C=C*H* 4.57 (H, d, J = 6.2 Hz, J_{H-Pt} = 63.6 Hz); H^5 7.32 (H, dd, J = 7.7 Hz, J = 5.5 Hz); H^f 7.48 (2H, m); H^3 7.55 (H, d, J = 6.2); H^4 7.86 (H, td, J = 6.2 Hz, J = 1.5 Hz); H^e 8.05 (2H, m); H^6 8.86 (H, d, J = 5.5 Hz, J_{H-Pt} = 30.3 Hz).

[Pt(η^2-tmetc)(N-SBu^t)]. Brown microcrystals (31% yield; t_{react} 19 h at 45 °C or 48 h at RT).

Found: C, 37.68; H, 4.32; N, 2.28; S, 5.21. $C_{20}H_{27}NO_8PtS$ requires: C, 37.74; H, 4.28; N, 2.20; S, 5.04.

IR (KBr pellets, cm^{-1}): $\nu_{C=N}$ 1605 (m); $\nu_{C=O}$ 1727 (s), 1703 (s).

^{1}H NMR (in CD_2Cl_2, RT), δ (ppm): C*H*$_3$ 1.43 (9H, s); OC*H*$_3$ 3.62 (3H,S); OC*H*$_3$ 3.65 (3H,S); C*H*$_2$S 4.35 (H, bs, J = 13.1 Hz); H^5 7.29 (H, dd, J = 7.7 Hz, J = 5.2 Hz); H^3 7.61 (H, d, J = 7.7 Hz); H^4 7.93 (H, dd, J = 7.7 Hz, J = 1.5 Hz); H^6 9.42 (H, d, J = 5.2 Hz, J_{H-Pt} = 30.1 Hz).

[Pt(η^2-fn)(N-SMe)]. Cream-coloured microcrystals (68% yield; t_{react} 4.5 h at 45 °C or 17 h at RT).

Found: C, 32.15; H, 2.80; N, 10.35; S, 7.71. $C_{11}H_{11}N_3PtS$ requires: C, 32.04; H, 2.69; N, 10.19; S, 7.78.

IR (KBr pellets, cm^{-1}): $\nu_{C=N}$ 1605 (m); $\nu_{C\equiv N}$ 2204 (s), 2195 (s).

^{1}H NMR (in $CDCl_3$, RT), δ (ppm): C*H*$_3$ 1.23 (3H, s); *H*C=C*H* 3.50 (H, d, J = 7.8 Hz, J_{H-Pt} = 82 Hz); *H*C=C*H* 3.94 (H, d, J = 7.8 Hz, J_{H-Pt} = 84 Hz); C*H*$_2$S 4.25 (2H, bs); H^5 7.36 (H, bt); H^3 7.67 (H, d, J = 7.7 Hz); H^4 8(H, td, J = 7.7 Hz, J = 1.5 Hz); H^6 8.27 (H, d, J = 6 Hz, J_{H-Pt} = 30 Hz).

[Pt(η^2-ma)(N-SPh)]. Cream-coloured microcrystals (63% yield; t_{react} 4 h at 45 °C.).

Found: C, 38.93; H, 2.73; N, 2.95; S, 6.52. $C_{16}H_{13}NO_3PtS$ requires: C, 38.87; H, 2.65; N, 2.83; S, 6.49.

IR (KBr pellets, cm^{-1}): $\nu_{C=N}$ 1603 (m); $\nu_{C=O}$ 1796 (s), 1730 (s).

^{1}H NMR (in $CDCl_3$, RT), δ (ppm): *H*C=C*H* 3.60 (H, d, J = 3.7 Hz, J_{H-Pt} = 82 Hz); *H*C=C*H* 3.94 (H, d, J = 3.7 Hz, J_{H-Pt} = 84 Hz); C*H*$_2$S 4.56 (2H, bs); H^5, H^b, H^d 7.31–7.38 (5H, m); H^3 7.57 (H, d, J = 7.7 Hz); H^c 7.64 (H, m); H^4 7.93 (H, td, J = 7.7 Hz, J = 1.6 Hz); H^6 9.20 (H, d, J = 4 Hz, J_{H-Pt} = 30 Hz)

[Pt(η^2-fn)(N-SPh)]. Cream-coloured microcrystals (47% yield; t_{react} 4 h at 45 °C or 17 h at RT).

Found: C, 40.58; H, 2.67; N, 8.97; S, 6.89. $C_{16}H_{13}N_3PtS$ requires: C, 40.50; H, 2.76; N, 8.86; S, 6.76.

IR (KBr pellets, cm^{-1}): $\nu_{C=N}$ 1605 (m); $\nu_{C\equiv N}$ 2201 (s).

^{1}H NMR (in $CDCl_3$, RT), δ (ppm): *H*C=C*H* 2.80 (H, d, J = 7.8 Hz, J_{H-Pt} = 90 Hz); *H*C=C*H* 3.06 (H, d, J = 7.8 Hz, J_{H-Pt} = 90 Hz); C*H*$_2$S 4.59 (2H, bs); H^5, H^b, H^d 7.30–7.41 (5H, m); H^3 7.57 (H, d, J = 6 Hz); H^c 7.72 (2H, bs); H^4 7.95 (H, td, J = 7.7, J = 1.6); H^6 7.28 (H, d, J = 6 Hz, J_{H-Pt} = 30 Hz).

[Pt(η^2-nq)(N-SPh)]. Brown microcrystals (53% yield; t_{react} 4 h at 45 °C).

Found: C, 47.77; H, 3.21; N, 2.41; S, 5.89. $C_{22}H_{17}NO_2PtS$ requires: C, 47.65; H, 3.09; N, 2.53; S, 5.78.

IR (KBr pellets, cm^{-1}): $\nu_{C=N}$ 1589 (m); $\nu_{C=O}$ 1639 (s).

^{1}H NMR (in $CDCl_3$, RT), δ (ppm): *H*C=C*H* 4.51 (H, d, J = 6.0 Hz, J_{H-Pt} = 72 Hz); C*H*$_2$S 4.47 (H, bs); *H*C=C*H* 4.63 (H, d, J = 6.0 Hz, J_{H-Pt} = 68 Hz); H^5, H^b, H^c 7.08–7.55 (5H, m); H^4 7.86 (H, t, J = 7.7 Hz); H^6 9.63 (H, d, J = 6.3 Hz, J_{H-Pt} = 31.2 Hz)

[Pt(η^2-tmetc)(N-SPh)]. Brown microcrystals (31% yield; t_{react} 23 h at RT).

Found: C, 40.37; H, 3.62; N, 2.24; S, 4.91. $C_{22}H_{23}NO_8PtS$ requires: C, 40.25; H, 3.53; N, 2.13; S, 4.88.

IR (KBr pellets, cm^{-1}): $\nu_{C=N}$ 1605 (m); $\nu_{C=O}$ 1728 (s), 1703 (s), 1693 (s).

^{1}H NMR (in $CDCl_3$, RT), δ (ppm): COOC*H*$_3$ 3.75 (6H, s); COOC*H*$_3$ 3.76 (6H,s); C*H*$_2$ S 4.58 (2H, m); H^5, H^3, H^b, H^c, H^e, H^f 7.35–7.75 (7H, m); H^4 7.86 (2H, t, J = 7.7Hz, J = 1.6 Hz); H^e 7.97 (2H, bs); H^f 8.11(2H, m); H^6 8.91 (H, d, J = 4 Hz, J_{H-Pt} = 31.5 Hz)

[Pt(η^2-ma)(N-N′C$_6$H$_4$OMe-4)]. Ochre microcrystals (53% yield; t_{react} 5 h at 45 °C).

Found: C, 40.52; H, 2.88; N, 5.46. $C_{17}H_{14}N_2O_4Pt$ requires: C, 40.40; H, 2.79; N, 5.54.

IR (KBr pellets, cm^{-1}): $\nu_{C=O}$ 1686 (s); $\nu_{C=N}$ 1597 (m).

^{1}H NMR (in $CDCl_3$, RT), δ (ppm): *H*C=C*H* 3.66 (H, d, J = 3.7 Hz, J_{H-Pt} = 83.4 Hz); *H*C=C*H* 3.71 (H, d, J = 3.7 Hz, J_{H-Pt} = 83.4 Hz); OCH$_3$ 3.91 (3H, s); H^1 7.07 (2H, d, J = 8.9); H^3, H^i 7.93–7.88 (H, m); H^5 7.65 (H, d, J = 7.7 Hz, J = 5.5 Hz); ^{4}H 8.17 (H, td, J = 6.21, J = 1.3); ^{6}H 9.25 (H, d, J = 5.5, J_{H-Pt} = 32); *H*C=N 9.27 (H, s, J_{H-Pt} = 56.9).

[Pt(η^2-fn)(N-N′C$_6$H$_4$OMe-4)]. Dark-red microcrystals (47% yield; t_{react} 4 h at 45 °C).

Found: C, 42.14; H, 2.89; N, 11.75. $C_{17}H_{14}N_4OPt$ requires: C, 42.06; H, 2.91; N, 11.54.

IR (KBr pellets, cm^{-1}): $\nu_{C=N}$ 1597 (m); $\nu_{C\equiv N}$ 2197 (s).

^{1}H NMR (in $CDCl_3$, RT), δ (ppm): *H*C=C*H* 2.75 (H, d, J = 7.7 Hz, J_{H-Pt} = 90 Hz); *H*C=C*H* 2.87 (H, d, J = 7.7 Hz, J_{H-Pt} = 92 Hz); PhOC*H*$_3$ 3.9 (3H, s); H^1 7.09 (2H, d, J = 5.1); H^5 7.68 (H, ddd, J = 6.7, J = 4.7, J = 1.3); H^3 7.94 (H, d, J = 7.94); H^i 7.90 (2H, d, J = 9.1); H^4 8.17 (H, td, J = 6.21, J = 1.3); H^6 9.28 (H, d, J = 5.7, J_{H-Pt} = 36); *H*C=N 9.27 (H, s, J_{H-Pt} = 28).

[Pt(η^2-dmf)(N-N′C$_6$H$_4$OMe-4)]. Brick-red microcrystals (67% yield; t_{react} 2.5 h at RT).

Found: C, 41.50; H, 3.75; N, 5.26. $C_{19}H_{20}N_2O_5Pt$ requires: C, 41.38; H, 3.66; N, 5.08.

IR (KBr pellets, cm^{-1}): $\nu_{C=N}$ 1597 (m); $\nu_{C=O}$ 1686 (s).

^{1}H NMR (in $CDCl_3$, RT), δ (ppm): *H*C=C*H* 3.74 (H, d, J = 8.8 Hz, J_{H-Pt} = 73.1 Hz); *H*C=C*H* 3.84 (H, d, J = 8.7 Hz, J_{H-Pt} = 9.28 Hz); PhOC*H*$_3$ 3.59 (3H, s); OC*H*$_3$ 3.67 (3H, s); OC*H*$_3$ 3.88 (3 H, s); H^1 6.90 (2H, d, J = 8.77); H^5 7.43 (H, bt); H^i 6.90 (2H, d, J = 8.77); H^3 7.94 (H, d, J = 7.68); H^4 8.06 (H, td, J = 6.21, J = 1.5); H^6 9.06 (H, bs); *H*C=N 9.31 (H, s, J_{H-Pt} = 53.7).

^{13}C NMR (in $CDCl_3$, RT), δ (ppm): H*C*=*C*H 24.91 (J_{C-Pt} = 415.0 Hz); H*C*=*C*H 25.99 (J_{C-Pt} = 387.0 Hz); O*C*H$_3$ 50.51; O*C*H$_3$ 50.81; PhO*C*H$_3$ 55.28; C^{i} 113.61; C^{i} 126.03 (J_{C-Pt} = 17.8 Hz); C^{5} 127.13 (J_{C-Pt} = 5.6 Hz); C^{3} 127.73 (J_{C-Pt} = 36.8 Hz); C^{4} 137.19; C^{m} 140.11; C^{6} 151.54 (J_{C-Pt} = 76.0 Hz); C^{h} 156.46; C^{2} 160.93; *C*=N 156.84; C^{2} 160.93; *C*=O 177.0 (J_{C-Pt} = 62.5); *C*=O 176.5 (J_{C-Pt} = 60.5).

[Pt(η^2-nq)(N-N′C$_6$H$_4$OMe-4)]. Brown microcrystals (81% yield; t_{react} 1 h at 40 °C).

Found: C, 48.66; H, 3.09; N, 5.09. $C_{23}H_{18}N_2O_3Pt$ requires: C, 48.85; H, 3.21; N, 4.95.

IR (KBr pellets, cm^{-1}): $\nu_{C=N}$ 1587 (m); $\nu_{C=O}$ 1632 (s).

^{1}H NMR (in $CDCl_3$, RT), δ (ppm): *H*C=C*H* 2.75 (H, d, J = 7.7 Hz, J_{H-Pt} = 90 Hz); *H*C=C*H* 2.87 (H, d, J = 7.7 Hz, J_{H-Pt} = 92 Hz); PhOC*H*$_3$ 3.9 (3H, s); H^{1} 7.09 (2H, d, J = 5.1); H^{5} 7.68 (H, ddd, J = 6.7, J = 4.7, J = 1.3); H^{3} 7.94 (H, d, J = 7.94); H^{i} 7.90 (2H, d, J = 9.1); ^{4}H 8.17 (H, td, J = 6.21, J = 1.3); ^{6}H 9.28 (H, d, J = 5.7, J_{H-Pt} = 36); *H*C=N 9.27 (H, s, J_{H-Pt} = 28).

[Pt(η^2-tmetc)(N-N′C$_6$H$_4$OMe-4)]. Ochre microcrystals (22% yield; t_{react} 22 h at RT).

Found: C, 41.39; H, 3.75; N, 4.33. $C_{23}H_{24}N_2O_9Pt$ requires: C, 41.38; H, 3.62; N, 4.20.

IR (KBr pellets, cm^{-1}): $\nu_{C=N}$ 1598 (m); $\nu_{C=O}$ 1696 (s).

^{1}H NMR (in $CDCl_3$, RT), δ (ppm): OC*H*$_3$ 3.63 (6H, s); OC*H*$_3$ 3.75 (6 H, s); PhOC*H*$_3$ 3.85 (3H, s); H^{1} 6.90 (2H, d, J = 10); H^{5} 7.50 (H, m); H^{3} 7.89 (H, d, J = 8); H^{4}–H^{i} 7.99–8.10 (3H, m); *H*C=N 9.18 (H, s, J_{H-Pt} = 56.3); ^{6}H 9.06 (H, d, J = 5.5, J_{H-Pt} = 24.9).

^{13}C NMR (in $CDCl_3$, RT), δ (ppm): *C*=*C* 41.39; *C*=*C* 41.50; O*C*H$_3$ 52.04; O*C*H$_3$ 52.35; PhO*C*H$_3$ 55.59; C^{l} 114.03; C^{i} 126.58; C^{5} 126.92; C^{3} 128.47 (J_{C-Pt} = 36.3 Hz); C^{4} 138.35; C^{6} 153.36 (J_{C-Pt} = 67.8 Hz); C^{h} 156.34; *C*=N 158.14; C^{2} 161.42; *C*=O 171.24; *C*=O 174.63.

[Pt(η^2-ma)(N-N′Bu^t)]. Ochre microcrystals (61% yield; t_{react} 3 h at RT).

Found: C, 36.77; H, 3.75; N, 6.23. $C_{14}H_{16}N_2O_3Pt$ requires: C, 36.93; H, 3.54; N, 6.15.

IR (KBr pellets, cm^{-1}): $\nu_{C=N}$ 1588 (m); $\nu_{C=O}$ 1795 (s); 1776 (s), 1720 (s).

^{1}H NMR (in $CDCl_3$, RT), δ (ppm): *H*C=C*H* 3.67 (H, d, J = 3.7 Hz, J_{H-Pt} = 82.6 Hz); *H*C=C*H* 3.74 (H, d, J = 3.7 Hz, J_{H-Pt} = 82.6 Hz); H^{5} (H, ddd, J = 6.7, J = 4.7, J = 1.3); H^{3} 7.83 (H, d, J = 6.0); H^{4} 8.13 (H, td, J = 8, J = 1.6); *H*C=N 9.00 (H, s, J_{H-Pt} = 62) H^{6} 9.25 (H, d, J = 4, J_{H-Pt} = 28).

^{13}C NMR (in $CDCl_3$, RT), δ (ppm): H*C*=*C*H 23.68 (J_{C-Pt} = 418.2 Hz); H*C*=*C*H 24.83 (J_{C-Pt} = 384.3 Hz); C–(*C*H$_3$)$_3$ 29.59 (J_{C-Pt} = 9.9); *C*-(CH$_3$)$_3$ 64.13; C^{5} 126.95 (J_{C-Pt} = 14.7 Hz); C^{3} 129.43 (J_{C-Pt} = 38.4 Hz); C^{4} 138.86; C^{6} 153.32 (J_{C-Pt} = 79.1 Hz); C^{2} 156.56; *C*=N 160.35; *C*=O 174.86; C=O 174.75.

[Pt(η^2-fn)(N-N′Bu^t)]. Ochre microcrystals (57% yield; t_{react} 3 h at RT).

Found: C, 38.51; H, 3.82; N, 12.99. $C_{14}H_{16}N_4Pt$ requires: C, 38.62; H, 3.70; N, 12.87.

IR (KBr pellets, cm^{-1}): $\nu_{C=N}$ 1593 (m); $\nu_{C=O}$ 2203 (s).

^{1}H NMR (in $CDCl_3$, RT), δ (ppm): C*H*$_3$ = 1.69 (9H, S); *H*C=C*H* 2.78 (H, d, J = 8.0 Hz, J_{H-Pt} = 90.6 Hz); *H*C=C*H* 2.83 (H, d, J = 8.0 Hz, J_{H-Pt} = 90.6 Hz); H^{5} 7.64(H, m); H^{3} 7.94 (H, d, J = 7.7); H^{4} (H, td, J = 7.6, J = 1.5); *H*C=N 9.01 (H, s, J_{H-Pt} = 60) H^{6} 9.29 (H, d, J = 4.7, J_{H-Pt} = 30).

^{13}C NMR (in $CDCl_3$, RT), δ (ppm): H*C*=*C*H −1.28 (J_{C-Pt} = 438.5 Hz); H*C*=*C*H 0.54 (J_{C-Pt} = 481.5 Hz); C–(*C*H$_3$)$_3$ 29.81; *C*-(CH$_3$)$_3$ 63.86; *C*≡N 124.16 (J_{C-Pt} = 72.3 Hz); C^{5} 126.50 (J_{C-Pt} = 13.6 Hz); C^{3} 129.06 (J_{C-Pt} = 37.3 Hz); C^{4} 138.54; C^{6} 153.25 (J_{C-Pt} = 78 Hz); C^{2} 156.15; *C*=N 159.74.

[Pt(η^2-dmf)(N-N′Bu^t)]. Ochre microcrystals (52% yield; t_{react} 4.5 h at RT).

Found: C, 38.25; H, 4.52; N, 5.51. $C_{16}H_{22}N_2O_4Pt$ requires: C, 38.32; H, 4.42; N, 5.59.

IR (KBr pellets, cm^{-1}): $\nu_{C=N}$ 1587 (m); $\nu_{C=O}$ 1680 (s).

^{1}H NMR (in $CDCl_3$, RT), δ (ppm): C*H*$_3$ = 1.63 (9H, S); *H*C=C*H* 3.68 (H, d, J = 8.8 Hz, J_{H-Pt} = 91.4 Hz); *H*C=C*H* 3.85 (H, d, J = 9.1 Hz, J_{H-Pt} = 91.4 Hz); H^{5} 7.55 (H, dd, J = 7.7, J = 1.5); H^{3} 7.69 (H, d, J = 7.7); H^{4} 8.06 (H, td, J = 7.6, J = 1.5); *H*C=N 9.00 (H, s, J_{H-Pt} = 57.0); H^{6} 9.31 (H, d, J = 4.7, J_{H-Pt} = 30.7).

^{13}C NMR (in $CDCl_3$, RT), δ (ppm): H*C*=*C*H 24.96 (J_{C-Pt} = 418.2 Hz); H*C*=*C*H 25.20 (J_{C-Pt} = 373.0 Hz); C–(*C*H$_3$)$_3$ 29.54; O*C*H$_3$ 50.38; O*C*H$_3$ 50.76; *C*-(CH$_3$)$_3$ 63.03; C^{5} 126.14; C^{3} 128.54 (J_{C-Pt} = 35.0 Hz); C^{4} 137.57; C^{6} 152.24 (J_{C-Pt} = 74.6 Hz); C^{2} 156.57; *C*=N 158.68; *C*=O 176.34; *C*=O 177.01.

[Pt(η^2-nq)(N-N′Bu^t)]. Dark-red microcrystals (72% yield; t_{react} 3 h at RT).

Found: C, 46.69; H, 3.81; N, 5.71. $C_{20}H_{20}N_2O_2Pt$ requires: C, 46.60; H, 3.91; N, 5.43.

IR (KBr pellets, cm^{-1}): $\nu_{C=N}$ 1585 (m), $\nu_{C=O}$ 1630 (s).

^{1}H NMR (in $CDCl_3$, RT), δ (ppm): C*H*$_3$ 1.53 (9H, s); *H*C=C*H* 4.50 (H, d, J = 6.2 Hz, J_{H-Pt} = 73.6 Hz); *H*C=C*H* 4.55 (H, d, J = 6.2 Hz, J_{H-Pt} = 73.1 Hz); H^{f} 7.45 (H, m); H^{5} 7.61 (H, dd, J = 6.7, J = 4.7, J = 1.3); H^{3} 7.73 (H, d, J = 7.7); H^{e}, H^{4} 8.02–8.09 (3H, m); *H*C=N 8.83 (H, s, J_{H-Pt} = 68.0); H^{6} 9.05 (H, d, J = 6.0, J_{H-Pt} = 30.4).

^{13}C NMR (in $CDCl_3$, RT), δ (ppm): C–(*C*H$_3$)$_3$ 29.31; H*C*=*C*H 41.54 (J_{C-Pt} = 372.99 Hz); H*C*=*C*H 42.95 (J_{C-Pt} = 308.6 Hz); *C*-(CH$_3$)$_3$ 64.22; C^{5} 126.25 (J_{C-Pt} = 13.6 Hz); C^{3} 128.68 (J_{C-Pt} = 35.0 Hz); C^{e} 124.9; C^{e} 125.3; C^{f} 130.86; C^{f} 130.95; C^{4} 138.09; C^{6} 150.19 (J_{C-Pt} = 63.3 Hz); C^{2} 156.55; *C*=N 158.66; C^{n} 186.94; C^{n} 177.01.

UV/vis, IR and NMR measurements

UV/vis spectra were recorded on a Perkin Elmer λ 40 spectrophotometer at the designed temperature. The reactions were studied by addition of known micro-aliquots of the entering olefin (ol$_2$) to a solution of the complex under study ([Pt]$_0$ ≈ 1 × 10^{-4} mol dm^{-3}) in $CHCl_3$ and recording spectral changes in the wavelength region 330–450 nm or at a suitable fixed wavelength.

The IR spectra and the ^{1}H and ^{13}C{^{1}H}-NMR spectra were recorded on a Nicolet Magna™ 750 spectrophotometer and on a Bruker AC™ 200 spectrometer, respectively.

The temperature-dependent ^{1}H-NMR spectra were analysed using the SWAN program.[13]

Mathematical and statistical data analysis were carried out on a personal computer equipped with a locally adapted version of Marquardt's algorithm.[14]

X-Ray structural analysis

All X-ray diffraction data collections were carried out on a NONIUS CAD-4 diffractometer equipped with an Oxford Cryostream liquid-N_2 device. Crystal data and details of measurements are reported in Table 4. Diffraction data were corrected for absorption by azimuthal scanning of high-χ reflections. The SHELX-97[15] package was used for structure solution and refinement based on F^2. ORTEP-3[16] was used for the graphical representation of the results. Common to all compounds: Mo Kα radiation, λ = 0.71069 Å, monochromator graphite. All non-H atoms in [Pt(η^2-ma)(N-N′Bu^t)] were refined anisotropically. In all cases hydrogen atoms were placed in calculated positions and thereafter allowed to ride on their parent atoms.

CCDC reference numbers 183322–183324.

See http://www.rsc.org/suppdata/dt/b2/b203085n/ for crystallographic data in CIF or other electronic format.

Table 4 Crystallographic data for complexes [Pt(η²-fn)(N-N′Bu^t)], [Pt(η²-ma)(N-N′Bu^t)] and [Pt(η²-dmf)(N-N′Bu^t)]

	[Pt(η²-fn)(N-N′Bu^t)]	[Pt(η²-ma)(N-N′Bu^t)]	[Pt(η²-dmf)(N-N′Bu^t)]
Empirical formula	$C_{14}H_{16}N_4Pt$	$C_{14}H_{16}N_2O_3Pt$	$C_{16}H_{22}N_2O_4Pt$
Formula weight	435.40	455.38	501.45
T/K	293(2)	293(2)	293(2)
System	Monoclinic	Monoclinic	Triclinic
Space group	$P2_1/a$	$P2_1/c$	$P\bar{1}$
Z	4	4	4
a/Å	9.338(2)	8.362(3)	8.969(3)
b/Å	8.706(2)	10.045(3)	12.776(4)
c/Å	18.463(3)	16.811(3)	15.380(4)
α/°			92.92(3)
β/°	96.046(17)	93.47(2)	95.15(2)
γ/°			94.92(3)
V/Å^3	1492.8(6)	1409.5(7)	1745.8(9)
μ(Mo Kα)/mm^{-1}	9.392	9.963	8.058
Measured reflections	2700	3812	6369
Unique reflections	2618	2465	6122
$R1$[on F, $I > 2\sigma(I)$]	0.0434	0.0276	0.0299
$wR2$ (F^2, all data)	0.1189	0.0656	0.0764

References

1 (*a*) F. Diederich and P. J. Stang, *Metal-Catalyzed Cross-Coupling Reactions*, ed. F. Diederich and P. J. Stang, Wiley-VCH, Weinheim, 1998; (*b*) M. J. Calhorda, J. M. Brown and N. A. Cooley, *Organometallics*, 1991, **10**, 1431; (*c*) K. Selvakumar, M. Valentini, P. S. Pregosin and A. Albinati, *Organometallics*, 1999, **18**, 4591; (*d*) R. F. Heck, *Acc. Chem. Res.*, 1979, **12**, 146; (*e*) R. F. Heck, *Comprehensive Organic Synthesis*, Pergamon, Oxford, 1991, vol. 4; (*f*) M. J. Brown and K. K. Hii, *Angew. Chem.*, 1996, **108**, 679; (*g*) M. J. Brown, *Chem. Soc. Rev.*, 1993, 25; (*h*) M. Tschoerner, P. S. Pregosin and A. Albinati, *Organometallics*, 1999, **18**, 670; (*i*) A. de Meijere and F. E. Meyer, *Angew. Chem.*, 1994, **106**, 2473; (*j*) A. Pfaltz, *Acta Chem. Scand.*, 1996, **50**, 189; (*k*) O. Reiser, *Angew. Chem.*, 1993, **105**, 576; (*l*) B. M. Trost and D. L. van Vranken, *Chem. Rev.*, 1996, **96**, 395; (*m*) L. Canovese, F. Visentin, P. Uguagliati, G. Chessa and A. Pesce, *J. Organomet. Chem.*, 1998, **566**, 61; (*n*) B. Crociani, S. Antonaroli, G. Bandoli, L. Canovese, F. Visentin and P. Uguagliati, *Organometallics*, 1999, **18**, 1137; (*o*) K. Selvakumar, M. Valentini, M. Wörle, P. S. Pregosin and A. Albinati, *Organometallics*, 1999, **18**, 1207; (*p*) K. Selvakumar, M. Valentini, P. S. Pregosin and A. Albinati, *Organometallics*, 1999, **18**, 4591.

2 (*a*) R. Van Asselt, C. J. Elsevier, W. J. J. Smeets and A. L. Speck, *Inorg. Chem.*, 1994, **33**, 1521; (*b*) P. T. Cheng, C. D. Cook, S. C. Nyburg and K. Y. Wan, *Inorg. Chem.*, 1971, **10**, 2210; (*c*) F. Ozawa, T. Ito, Y. Nakamura and A. Yamamoto, *J. Organomet. Chem.*, 1979, **168**, 375; (*d*) R. Van Asselt and C. J. Elsevier, *Tetrahedron*, 1994, **50**, 323; (*e*) F. Gomez-de la Torre, F. A. Jalon, A. Lopez-Agenjo, B. R. Manzano, A. Rodriguez, T. Sturm, W. Weissensteiner and M. Martinez-Ripoll, *Organometallics*, 1998, **17**, 4634; (*f*) M. Tschoerner, G. Trabesinger, A. Albinati and P. S. Pregosin, *Organometallics*, 1997, **16**, 3447.

3 (*a*) L. Canovese, F. Visentin, P. Uguagliati and B. Crociani, *J. Chem. Soc., Dalton Trans.*, 1996, 1921; (*b*) L. Canovese, F. Visentin, G. Chessa, P. Uguagliati and A. Dolmella, *J. Organomet. Chem.*, 2000, **601**, 1; (*c*) L. Canovese, F. Visentin, G. Chessa, G. Gardenal and P. Uguagliati, *J. Organomet. Chem.*, 2001, **622**, 155.

4 L. Canovese, V. Lucchini, C. Santo, F. Visentin and A. Zambon, *J. Organomet. Chem.*, 2002, **642**, 58.

5 P. Uguagliati, R. A. Michelin, U. Belluco and R. Ros, *J. Organomet. Chem.*, 1979, **169**, 115.

6 Z. G. Szabó, in *Chemical Kinetics*, ed. C. H. Bamford and C. F. H. Tipper, Elsevier, Amsterdam, 1969, vol. 2, ch. 1.

7 F. H. Allen and O. Kennard, *Chem. Des. Autom. News*, 1993, **8**, 31.

8 V. G. Albano, C. Castellari, M. Monari, V. De Felice, A. Panunzi and F. Ruffo, *Organometallics*, 1996, **15**, 4012.

9 L. Canovese, F. Visentin, P. Uguagliati, G. Chessa and A. Pesce, *J. Organomet. Chem.*, 1998, **566**, 61.

10 B. Crociani, F. Di Bianca, P. Uguagliati, L. Canovese and A. Berton, *J. Chem. Soc., Dalton Trans.*, 1991, 71.

11 D. D. Perrin and W. L. F. Armarego, *Purification of Laboratory Chemicals*, Pergamon Press, Oxford, 4th edn., 1998.

12 K. Moseley and P. M. Maitlis, *J. Chem. Soc., Dalton Trans.*, 1974, 169.

13 G. Balacco, *J. Chem. Inf. Comput. Sci.*, 1994, **34**, 1235.

14 D. W. Marquardt, *SIAM J. Appl. Math.*, 1963, **11**, 431.

15 G. M. Sheldrick, SHELXL97, Program for Crystal Structure Determination, University of Göttingen, Göttingen, Germany, 1997.

16 L. J. Farrugia, *J. Appl. Cryst.*, 1997, **30**, 565.